Article

CO$_2$ Reduction Using Water as an Electron Donor over Heterogeneous Photocatalysts Aiming at Artificial Photosynthesis

Published as part of the Accounts of Chemical Research special issue "CO$_2$ Reductions via Photo and Electrochemical Processes".

Shunya Yoshino, Tomoaki Takayama, Yuichi Yamaguchi, Akihide Iwase, and Akihiko Kudo*

Read Online

ACCESS | Metrics & More | Article Recommendations

CONSPECTUS: Photocatalytic and photoelectrochemical CO$_2$ reduction of artificial photosynthesis is a promising chemical process to solve resource, energy, and environmental problems. An advantage of artificial photosynthesis is that solar energy is converted to chemical products using abundant water as electron and proton sources. It can be operated under ambient temperature and pressure. Especially, photocatalytic CO$_2$ reduction employing a powdered material would be a low-cost and scalable system for practical use because of simplicity of the total system and simple mass-production of a photocatalyst material.

In this Account, single particulate photocatalysts, Z-scheme photocatalysts, and photoelectrodes are introduced for artificial photosynthetic CO$_2$ reduction. It is indispensable to use water as an electron donor (i.e., reasonable O$_2$ evolution) but not to use a sacrificial reagent of a strong electron donor, for achievement of the artificial photosynthetic CO$_2$ reduction accompanied by $\Delta G > 0$. Confirmations of O$_2$ evolution, a ratio of reacted e$^-$ to h$^+$ estimated from obtained products, a turnover number, and a carbon source of a CO$_2$ reduction product are discussed as the key points for evaluation of photocatalytic and photoelectrochemical CO$_2$ reduction. Various metal oxide photocatalysts with wide band gaps have been developed for water splitting under UV light irradiation. However, these bare metal oxide photocatalysts without a cocatalyst do not show high photocatalytic CO$_2$ reduction activity in an aqueous solution. The issue comes from lack of a reaction site for CO$_2$ reduction and competitive reaction between water and CO$_2$ reduction. This raises a key issue to find a cocatalyst and optimize reaction conditions defining this research field. Loading a Ag cocatalyst as a CO$_2$ reduction site and NaHCO$_3$ addition for a smooth supply of hydrated CO$_2$ molecules as reactant are beneficial for efficient photocatalytic CO$_2$ reduction. Ag/BaLa$_4$Ti$_4$O$_{15}$ and Ag/NaTaO$_3$:Ba reduce CO$_2$ to CO as a main reduction reaction using water as an electron donor even in just water and an aqueous NaHCO$_3$ solution. A Rh−Ru cocatalyst on NaTaO$_3$:Sr gives CH$_4$ with 10% selectivity (Faradaic efficiency) based on the number of reacted electrons in the photocatalytic CO$_2$ reduction accompanied by O$_2$ evolution by water oxidation.

Visible-light-responsive photocatalyst systems are indispensable for efficient sunlight utilization. Z-scheme systems using CuGaS$_2$, (CuGa)$_{1−x}$Zn$_{2x}$S$_2$, CuGa$_{1−x}$In$_x$S$_2$, and SrTiO$_3$:Rh as CO$_2$-reducing photocatalyst, BiVO$_4$ as O$_2$-evolving photocatalyst, and reduced graphene oxide (RGO) and Co-complex as electron mediator or without an electron mediator are active for CO$_2$ reduction using water as an electron donor under visible light irradiation. These metal sulfide photocatalysts have the potential to take part in Z-scheme systems for artificial photosynthetic CO$_2$ reduction, even though their ability to extract electrons from water is insufficient. A photoelectrochemical system using a photocathode is also attractive for CO$_2$ reduction under visible light irradiation. For example, p-type CuGaS$_2$, (CuGa)$_{1−x}$Zn$_{2x}$S$_2$, Cu$_{1−x}$Ag$_x$GaS$_2$, and SrTiO$_3$:Rh function as photocathodes for CO$_2$ reduction under visible light irradiation. Moreover, introducing a conducting polymer as a hole transporter and surface modification with Ag and ZnS improve photoelectrochemical performance.
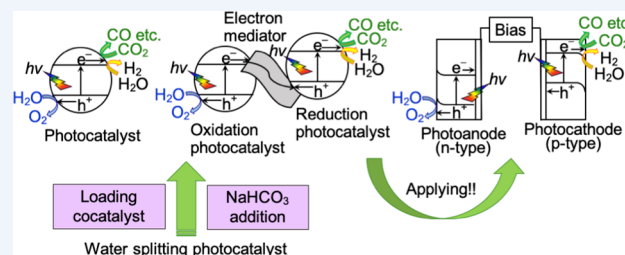
◼ KEY REFERENCES

- Iizuka, K.; Wato, T.; Miseki, Y.; Saito, K.; Kudo, A. Photocatalytic Reduction of Carbon Dioxide over Ag Cocatalyst-Loaded ALa$_4$Ti$_4$O$_{15}$ (A = Ca, Sr, and Ba) Using Water as a Reducing Reagent. *J. Am. Chem. Soc.* **2011**, *133*, 20863−20868.[1] Ag-cocatalyst for an effective
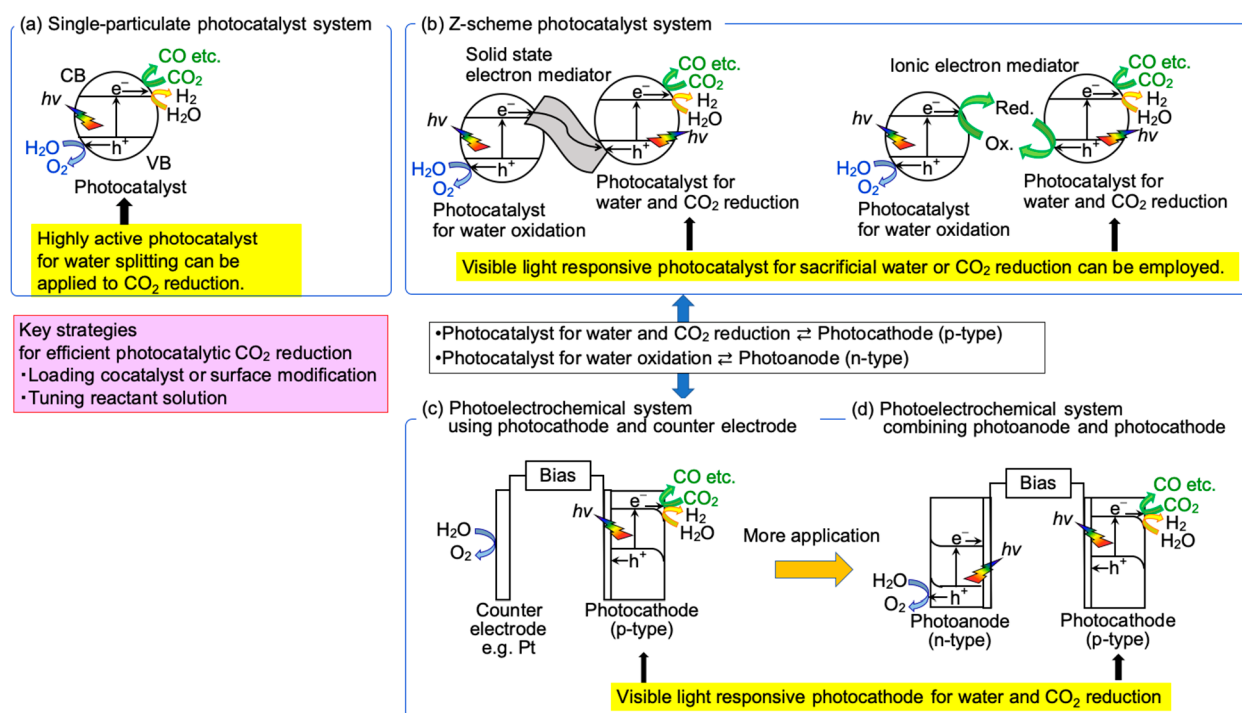
Figure 1. Artificial photosynthetic CO_2 reduction based on a powdered photocatalyst by (a) a single-particulate system, (b) a Z-scheme system, (c) a photoelectrochemical system using a photocathode, and (d) a photoelectrochemical system combining a photocathode and a photoanode.

active site for CO_2 reduction and $Ag/BaLa_4Ti_4O_{15}$ photocatalyst for CO_2 reduction to form CO as a main reduction product using water as an electron donor even in an aqueous solution.

- Nakanishi, H.; Iizuka, K.; Takayama, T.; Iwase, A.; Kudo, A. Highly Active $NaTaO_3$-Based Photocatalysts for CO_2 Reduction to Form CO Using Water as the Electron Donor. *ChemSusChem* **2017**, *10*, 112−118.[2] $Ag/NaTaO_3$ photocatalyst doped with alkaline earth cations for CO_2 reduction to CO with 90% of selectivity in an aqueous solution with a basic salt for enhancement of hydrated CO_2 molecules supply.

- Iwase, A.; Yoshino, S.; Takayama, T.; Ng, Y. H.; Amal, R.; Kudo, A. Water Splitting and CO_2 Reduction under Visible Light Irradiation Using Z-Scheme Systems Consisting of Metal Sulfides, CoO_x-Loaded $BiVO_4$, and a Reduced Graphene Oxide Electron Mediator. *J. Am. Chem. Soc.* **2016**, *138*, 10260−10264.[3] Z-scheme system composed of $CuGaS_2$ as a reducing photocatalyst and $RGO−(CoO_x/BiVO_4)$ as an O_2-evolving photocatalyst for CO_2 reduction to CO using water as an electron donor under visible light irradiation in an aqueous powder suspension system.

- Yoshino, S.; Iwase, A.; Yamaguchi, Y.; Suzuki, T. M.; Morikawa, T.; Kudo, A. Photocatalytic CO_2 Reduction Using Water as an Electron Donor under Visible Light Irradiation by Z-Scheme and Photoelectrochemical Systems over $(CuGa)_{0.5}ZnS_2$ in the Presence of Basic Additives. *J. Am. Chem. Soc.* **2022**, *144*, 2323−2332.[4] Employing $(CuGa)_{0.5}ZnS_2$ prepared by a flux method in Z-scheme and photoelectrochemical systems with tuning a reactant solution for efficient and stable CO_2 reduction to form CO with 10−20% selectivity using water as an electron donor under visible light.

1. INTRODUCTION

Carbon dioxide capture storage and utilization technology (CCSU) has been encouraged, because CO_2 emission control is a critical issue in the world. Ideally, CO_2 fixation should be realized utilizing renewable energies, such as solar energy, as follows:

- hydrogenation of CO_2 using solar hydrogen
- biological CO_2 fixation
- electrochemical CO_2 reduction utilizing a photovoltaic cell
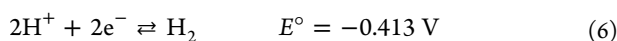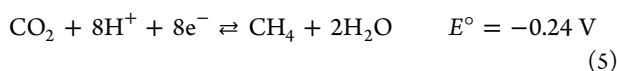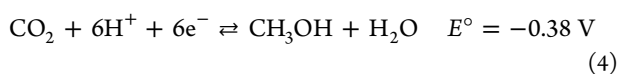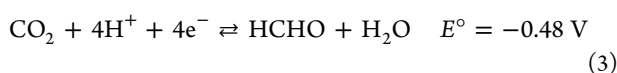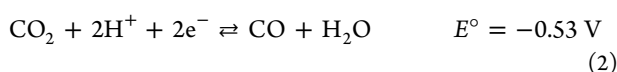- photocatalytic and photoelectrochemical CO_2 reduction directly utilizing solar light

There are advantages and disadvantages to each reaction. Hydrogenation of CO_2 can produce various beneficial chemical compounds with high CO_2 conversion efficiency through a thermal catalytic process on an industrial scale. Much knowledge toward CO_2 hydrogenation has been accumulated in C1 chemistry so far. The hydrogen should be supplied from solar hydrogen production by water splitting with no consumption of fossil resources and no CO_2 emission but not from steam reforming of fossil resources. However, the CO_2 conversion process requires high temperature and pressure to operate the catalytic process. Biological CO_2 fixation is based on natural photosynthesis by plants. Natural photosynthesis involves almost no energy loss for absorbed photon energy conversion. However, the solar energy conversion efficiency is limited because a plant absorbs only a part of the solar spectrum as indicated by its green color. Electrochemical CO_2 reduction is also interesting from the viewpoint of electrocatalysis. The reduction products and the selectivity change with electrode materials even under the same electrolysis conditions. However, electrolyzers and batteries are indispensable for the electrochemical system in addition to a photovoltaic cell. Photocatalytic and photoelectrochemical

CO_2 reduction utilizing solar energy in an aqueous solution is one of the ideal chemical reactions for artificial photosynthesis, because solar energy is directly converted and stored as chemical products. Artificial photosynthesis can be operated under ambient temperature and pressure to produce solar fuels and chemicals and can exceed natural photosynthesis in solar energy conversion efficiency. Especially, a powder-based photocatalyst is attractive because it can be employed for a low-cost and scalable system aimed at artificial photosynthesis.[5]

In this Account, we introduce several types of CO_2 reduction systems, mainly based on particulate photocatalyst materials, using water as an electron donor. Key points for evaluation of photocatalytic and photoelectrochemical CO_2 reduction are also discussed.

2. OVERVIEW OF PHOTOCATALYTIC AND PHOTOELECTROCHEMICAL CO_2 REDUCTION SYSTEMS FOR ARTIFICIAL PHOTOSYNTHESIS

Figure 1 shows various types of photocatalytic and photo-electrochemical systems for artificial photosynthesis.[6,7] The first is a single-particulate photocatalyst system via one-photon excitation, in which photocatalytic reduction by photo-generated electrons and photocatalytic oxidation by photo-generated holes proceed on one particle (Figure 1a).[6−9] Photocatalysts of semiconductor materials have a band structure in which a conduction band (CB) is separated from a valence band (VB) with a band gap (BG). The thermodynamic relationship between the band structure of a photocatalyst and the redox potential for the objective reaction is important. The equilibrium potentials relative to the normal hydrogen electrode (NHE) at pH 7 and 298 K for CO_2 reduction and water splitting are as follows:

$$CO_2 + 2H^+ + 2e^- \rightleftarrows HCOOH \qquad E° = -0.61 \text{ V} \tag{1}$$

$$CO_2 + 2H^+ + 2e^- \rightleftarrows CO + H_2O \qquad E° = -0.53 \text{ V} \tag{2}$$

$$CO_2 + 4H^+ + 4e^- \rightleftarrows HCHO + H_2O \quad E° = -0.48 \text{ V} \tag{3}$$

$$CO_2 + 6H^+ + 6e^- \rightleftarrows CH_3OH + H_2O \quad E° = -0.38 \text{ V} \tag{4}$$

$$CO_2 + 8H^+ + 8e^- \rightleftarrows CH_4 + 2H_2O \qquad E° = -0.24 \text{ V} \tag{5}$$

$$2H^+ + 2e^- \rightleftarrows H_2 \qquad E° = -0.413 \text{ V} \tag{6}$$

$$O_2 + 4H^+ + 4e^- \rightleftarrows 2H_2O \qquad E° = +0.817 \text{ V} \tag{7}$$

The conduction band minimum and valence band maximum should locate at more negative and positive levels than redox potentials of objective reactions such as water splitting and CO_2 reduction, respectively. When the energy of the incident photon is larger than that of the band gap, electrons and holes are photogenerated in the conduction band and the valence band, respectively. The photogenerated electrons reduce water and CO_2 to generate H_2 and CO_2 reduction products such as CO, while the photogenerated holes oxidize water to form O_2. The O_2 evolution is a key issue for photocatalytic CO_2 reduction using water as an electron donor. Moreover, since CO_2 reduction competes with water reduction, selective CO_2

reduction is also challenging from the viewpoints of not only thermodynamics but also kinetics. Therefore, the catalytic ability of photocatalyst surface is also a key issue.

The second is a Z-scheme system via a two-photon excitation process consisting of a reducing photocatalyst, an oxidizing photocatalyst, and an electron mediator (Figure 1b).[10−13] This system mimics natural photosynthesis by a plant. Various photocatalysts that are active for either photocatalytic reduction of water and CO_2 reduction or photocatalytic oxidation of water can be employed to make a Z-scheme system. From this viewpoint, it is meaningful to test photocatalytic CO_2 reduction using sacrificial electron donors such as organic compounds and S^{2-} in order to find potential CO_2-reducing photocatalysts in a part of the Z scheme system, though the sacrificial reaction becomes a downhill reaction ($\Delta G < 0$).

The third is a photoelectrochemical cell.[7] n-Type and p-type semiconductors may function as O_2-evolving photoanodes and photocathodes to give H_2 and reduction products of CO_2, respectively. The photoelectrochemical cell can be constructed by combining a photoelectrode of a working electrode with a counter electrode (Figure 1c) or combining a photoanode and a photocathode working via two-photon excitation (Figure 1d). External bias can be applied between the photoanode and photocathode to enhance the photoelectrochemical reaction. However, the external bias should be smaller than the theoretical voltage of electrolysis of an objective reaction to achieve artificial photosynthesis from light energy conversion.

In the following sections, several types of the photocatalytic and photoelectrochemical systems shown in Figure 1 are introduced.

3. SINGLE PARTICULATE PHOTOCATALYSTS WITH WIDE BAND GAPS FOR CO_2 REDUCTION USING WATER AS AN ELECTRON DONOR (FIGURE 1a)

3.1. Ag Cocatalyst for CO Formation by Photocatalytic CO_2 Reduction

CO_2 reduction over metal oxide photocatalysts has extensively been investigated. Although TiO_2 has widely been studied for photocatalytic CO_2 reduction, those reports involve critical issues such as lack of quantification of O_2 and small amounts of reduction products such as CH_4 due to low activities. Ishitani et al. reported that CH_4 could come from contaminants adsorbed on TiO_2.[14] In contrast, Sayama and Arakawa have reported that a ZrO_2 photocatalyst (BG = 5.0 eV) produced CO, H_2, and O_2 in stoichiometric amounts in an aqueous medium.[15] Moreover, loading a Cu cocatalyst and adding a bicarbonate ion enhanced the photocatalytic CO_2 reduction. This is the first report to demonstrate photocatalytic CO_2 reduction using water as an electron donor over a particulate photocatalyst. However, the major reduction product was H_2 and the selectivity for CO formation ($CO/(H_2 + CO)$) was about 12%. In such a background, the author found a highly active Ag cocatalyst for photocatalytic CO_2 reduction to form CO with highly active photocatalysts for water splitting.

$BaLa_4Ti_4O_{15}$ (BG = 3.9 eV) photocatalyst with a layered perovskite structure was first chosen because $NiO_x/BaLa_4Ti_4O_{15}$ efficiently split water.[16] The particle is plate shaped in which an edge plane and a basal plane are reduction and oxidation site, respectively, as shown in Figure 2A. The separation of the reduction site from the oxidation site is beneficial for an uphill reaction, because a back reaction of a
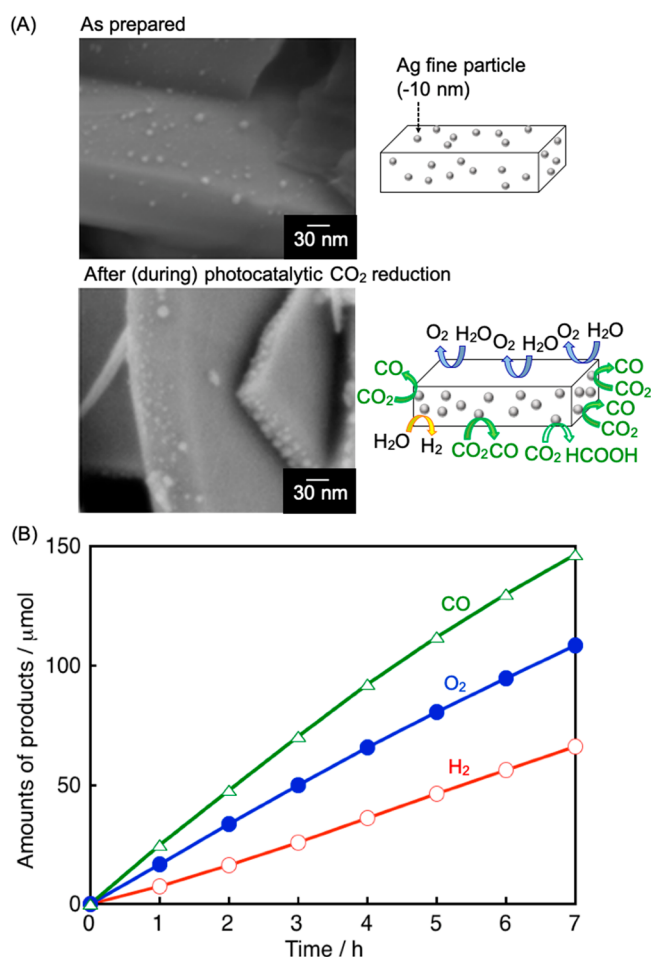
(A)

(B)

Figure 2. (A) SEM images of $Ag/BaLa_4Ti_4O_{15}$ before and after photocatalytic CO_2 reduction, and the proposed mechanism. (B) Photocatalytic CO_2 reduction using water as an electron donor under UV light irradiation over $Ag(2\ wt\ \%)/BaLa_4Ti_4O_{15}$.[1] Photocatalyst, 0.3 g; reactant solution, water (360 mL); flow gas, CO_2 (1 atm); light source, 400 W high-pressure mercury lamp; reaction cell, inner irradiation quartz cell. Reproduced with permission from ref 1. Copyright 2011 American Chemical Society.

downhill reaction is suppressed. Ag was found to be a highly active cocatalyst for photocatalytic CO_2 reduction to form CO as shown in Table 1.[1] To compare photocatalytic CO_2 reduction abilities, not only the production rate [mol h^{-1}]

but also the selectivity for CO_2 reduction are essential values. The selectivity is calculated according to eq 8.

$$\text{selectivity [\%]} = 100 \times (\text{number of electrons reacted for}$$
$$\text{objective production})$$
$$/(\text{sum of all reacted electrons}) \qquad (8)$$

The selectivity and the production rate based on the number of reacted electrons are similar to Faradaic efficiency and partial current density, respectively, in an electrochemical reaction. It is noteworthy that CO is the main reduction product with about 70% selectivity, rather than H_2, even in an aqueous medium (Table 1). A small amount of HCOOH was also obtained. It is reasonable that Ag functions as an efficient cocatalyst to form CO judging from its electrocatalysis in aqueous CO_2 solution.[17,18] The high conduction band level of $BaLa_4Ti_4O_{15}$ should be important to get an enough driving force for CO_2 reduction and high energy potential of photogenerated electrons applied to the Ag cocatalyst. A liquid-phase reduction method gives higher activity for CO formation than photodeposition and impregnation methods for the Ag cocatalyst loading. There is concern that the Ag cocatalyst may efficiently reduce O_2 produced by water splitting. However, O_2 reduction on the Ag cocatalyst is suppressed more or less, because the reaction is conducted under CO_2 flow conditions smoothly removing the O_2 from the reaction system.

Figure 2A shows SEM images of Ag-cocatalyst before and after photocatalytic CO_2 reduction and a reaction mechanism. $BaLa_4Ti_4O_{15}$ is a plate-like particle with layered perovskite structure. Ag particles of ~10 nm diameter are loaded on both edge and basal plane by the liquid-phase reduction as prepared. After photocatalytic CO_2 reduction, the number of the Ag cocatalyst particles on the edge increases while Ag particles on the basal plane disappear, because Ag on the basal plane dissolves by photooxidation and is subsequently photodeposited on the edge by photoreduction during the photocatalytic CO_2 reduction.

Figure 2B shows time courses of CO, H_2, and O_2 evolution by photocatalytic CO_2 reduction over $Ag/BaLa_4Ti_4O_{15}$. The time courses demonstrate not only activity and durability but also other important points to evaluate photocatalytic CO_2 reduction as discussed below.

It is important to see if O_2 evolves in a stoichiometric amount when the photocatalytic reaction is conducted using

Table 1. Effect of Cocatalyst on CO_2 Reduction Using Water as an Electron Donor under UV Light Irradiation over $BaLa_4Ti_4O_{15}$ Photocatalyst[1a]

		activity [μmol h^{-1}]					
cocatalyst (wt %)	loading method	H_2	O_2	CO	HCOOH	CO selectivity (%)	e$^-$/h$^+$
none		5.3	2.4	0	0	0	1.1
NiO_x (0.5)	impregnation[b]	58	29	0.02	0	0.03	1.0
Ru (0.5)	photodeposition	84	41	0	0	0	1.0
Cu (0.5)	photodeposition	96	45	0.6	0	0.6	1.1
Au (0.5)	photodeposition	110	51	0	0	0	1.1
Ag (1.0)	photodeposition	10	7.0	4.3	0.3	30	1.0
Ag (1.0)	impregnation	8.2	5.7	5.2	0.2	38	1.2
Ag (1.0)	impregnation + H_2 reduction	5.6	8.7	8.9	0.3	60	0.9
Ag (1.0)	liquid-phase reduction	5.6	12	19	0.4	76	1.0

[a]Photocatalyst, 0.3 g; reactant solution, water (360 mL); flow gas, CO_2 (1 atm); light source, 400 W high-pressure mercury lamp; reaction cell, inner irradiation quartz cell. [b]Treated with H_2 reduction and subsequent oxidation.
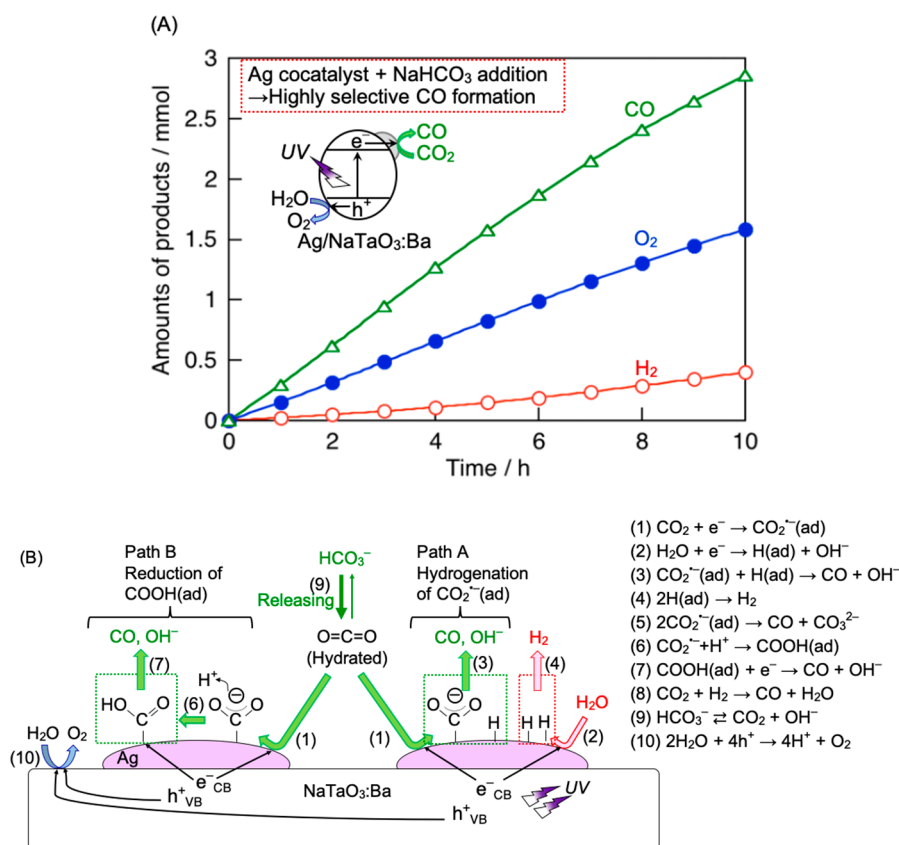
Figure 3. (A) Photocatalytic CO_2 reduction using water as an electron donor under UV light irradiation over $Ag/NaTaO_3$:Ba. Reactant solution, $NaHCO_{3(aq)}$ (360 mL); flow gas, CO_2 (1 atm); light source, 400 W high-pressure mercury lamp; reaction cell, an inner irradiation quartz cell. (B) Proposed mechanism of photocatalytic CO_2 reduction in the presence of $NaHCO_3$.[2] Reproduced with permission from ref 2. Copyright 2017 Wiley.

water as an electron donor for light energy conversion without any strong sacrificial electron donors. CO_2 is reduced by photogenerated electrons on a photocatalyst, while photocatalytic oxidation of water by photogenerated holes simultaneously proceeds as the counterpart as shown in Figures 1a and 2B. It is also important to see if the ratio of reacted electrons to holes estimated from products is unity according to eq 9.

$$e^-/h^+ = (\text{number of reacted electrons calculated from}$$
$$\text{reduction products})/(\text{number of reacted holes}$$
$$\text{calculated from oxidation products}) \quad (9)$$

Unity means that reduction and oxidation products are obtained in a stoichiometric amount. If the e^-/h^+ is not unity, side reactions or noncatalytic but quantitative reactions such as reduction or oxidation of the photocatalyst itself may proceed. In addition, it is necessary to pay attention to whether some products are not detected by the measurement technique employed. The O_2 evolution with at unity e^-/h^+ ratio is satisfied for the present photocatalytic CO_2 reduction over $Ag/BaLa_4Ti_4O_{15}$ as shown in Table 1 and Figure 2B.

Photocatalytic reaction must proceed by irradiation the energy of which is larger than the band gap energy. The band gap of $BaLa_4Ti_4O_{15}$ is 3.9 eV, which corresponds to about 320 nm light. This photocatalyst works with use of a quartz reaction cell with a suitable UV lamp, while the activity is negligible using a Pyrex reaction cell. This result indicates that

the photoresponse of the $BaLa_4Ti_4O_{15}$ photocatalyst is reasonable.

Turnover number defined by eq 10 is also an important indicator to consider if the reaction proceeds photocatalytically.

$$[\text{TON}] = [\text{molar quantity of products}]$$
$$/[\text{molar quantity of active sites}] \quad (10)$$

Turnover number (TON) indicates how many atoms or molecules react on one active site. TON based on the number of reacted electrons is often used for photocatalysis accompanied by redox reactions according to eq 11.

$$[\text{TON}] = [\text{number of reacted electrons for objective}$$
$$\text{production}]/[\text{number of active sites}]$$
$$= [\text{molar quantity of reacted electrons for objective}$$
$$\text{production}]/[\text{molar quantity of an employed}$$
$$\text{photocatalyst}] \quad (11)$$

If the TON is too small, we cannot guarantee that it is a photocatalytic reaction because not catalytic but quantitative reactions on the surface of photocatalyst cannot be excluded. In a heterogeneous photocatalyst, the molar quantity of the active site is often replaced with the molar quantity of an employed photocatalyst, because it is difficult to estimate the number of actual active sites on the surface of a photocatalyst.

Table 2. Single Particulate Photocatalysts with Wide Band Gaps for CO_2 Reduction Using Water as an Electron Donor[1,2,22−24a]

photocatalyst	BG [eV]	crystal structure	Ag cocatalyst (wt %, loading method)	additive	activity [μmol h^{-1}]			CO selectivity (%)
					H_2	O_2	CO	
$CaLa_4Ti_4O_{15}$	3.9	layered perovskite	Ag (1.0, LPR)	none	3.2	6.6	9.3	72
$SrLa_4Ti_4O_{15}$	3.8	layered perovskite	Ag (1.0, LPR)	none	4.8	5.8	7.1	56
$BaLa_4Ti_4O_{15}$	3.9	layered perovskite	Ag (1.0, LPR)	none	5.6	12	19	76
$K_4Nb_6O_{17}$	3.4	layered	Ag(3.0, LPR)	$NaHCO_3$	11	9	8	42
$NaTaO_3$	4.0	perovskite	Ag(1.0, PD)	none	32	16	1.4	4.2
$NaTaO_3$:Ba	4.1	perovskite	Ag(3.0, LPR)	$NaHCO_3$	24	76	125	84
$NaTaO_3$:Sr	4.1	perovskite	Ag(2.0, LPR)	$NaHCO_3$	28	102	176	86
$NaTaO_3$:Ca	4.1	perovskite	Ag(2.0, LPR)	$NaHCO_3$	15	84	148	91
$AgTaO_3$	3.4	perovskite	none	$NaHCO_3$	27	15	4.2	13
$KCaSrTa_5O_{15}$	4.1	tungsten bronze	Ag(0.5, Imp)	$NaHCO_3$	15	46	97	87
$K_3Ta_3B_2O_{12}$	4.0	tungsten bronze like	Ag(2.0, PD)	$NaHCO_3$	55	32	16.7	23
$SrTa_2O_6$	4.4	$CaTa_2O_6$	Ag(3.0, LPR)	$NaHCO_3$	95	86	87	48
$BaTa_2O_6$	4.1	$CaTa_2O_6$ as main phase	Ag(2.0, LPR)	$NaHCO_3$	30	16	7	19
$LaTa_7O_{19}$	4.1	laminate	Ag(1.0, Imp)	$NaHCO_3$	9	17	25	74
$CaTa_4O_{11}$	4.5	laminate	Ag(1.0, Imp)	$NaHCO_3$	31	30	35	53

[a]Photocatalyst, 0.3−1.5 g; reactant solution, water (350−360 mL); flow gas, CO_2 (1 atm); light source, 400 W high-pressure mercury lamp; reaction cell, inner irradiation quartz cell. PD, photodeposition; LPR, liquid-phase reduction; Imp, impregnation.

In some cases, the molar quantities of atoms on the surface, dopant, and cocatalyst are used for the denominator. The TON should be above unity to prove that the reaction proceeds catalytically. Photocatalytic CO_2 reduction over Ag/$BaLa_4Ti_4O_{15}$ proceeds steadily under UV light irradiation and TON to photocatalyst and cocatalyst reach 1.6 and 7.7, respectively, at 7 h being above unity as shown in Figure 2B.

Products of CO and HCOOH among others must originate from CO_2. However, contaminants on the photocatalyst and some carbon materials constituting the photocatalyst system may become a carbon source.[14,19] Therefore, confirmation of the carbon source of the obtained products is necessary. One approach is an isotope experiment using $^{13}CO_2$. Another is a control experiment using an inert gas to confirm that carbon products are not obtained. The reactant solution conditions (i.e., pH) of the control experiment should be similar to those of CO_2 reduction. When $^{13}CO_2$ is flowed for a photocatalytic reaction over Ag/$BaLa_4Ti_4O_{15}$, ^{13}CO is obtained while ^{12}CO is not. In addition, CO is not obtained when Ar instead of CO_2 is supplied. These two results prove CO_2 is the carbon source.

Thus, it is concluded by confirmations of O_2 evolution, the ratio of reacted e$^-$ to h$^+$ estimated from obtained products, the TON, and the carbon source that the CO_2 reduction photocatalytically proceeds using water as an electron donor over Ag/$BaLa_4Ti_4O_{15}$.

3.2. Effect of HCO_3^- in Water on Photocatalytic CO_2 Reduction

La or alkaline earth metal doped $NaTaO_3$ (BG = 4.1 eV) with a perovskite structure is also a unique photocatalyst. The doped $NaTaO_3$ has a surface nanostep structure in which a reduction site is separated from an oxidation site.[20,21] While NiO/$NaTaO_3$ with dopant splits water efficiently but does not reduce CO_2, Ag/$NaTaO_3$:Ba gives CO with about 50% selectivity under UV light upon flowing CO_2 into pure water.[2] Moreover, with addition of a basic salt into the reactant solution, CO formation rate drastically increases and the selectivity reaches about 90% even in an aqueous solution (Figure 3A). The enhancement of CO_2 reduction with salt

addition is due to efficient supply of hydrated CO_2 molecule reactant and pH control.

A proposed mechanism of photocatalytic CO_2 reduction over Ag/$NaTaO_3$:Ba in the presence of a basic additive is shown in Figure 3B. It was confirmed that not HCO_3^- or CO_3^{2-} but a hydrated CO_2 molecule is a reactant in photocatalytic CO_2 reduction as in electrochemical CO_2 reduction. HCO_3^- functions as a buffer for supply of hydrated CO_2 molecules. After the CO_2 adsorbs on the Ag-cocatalyst to make $CO_2^{\bullet-}{}_{(ad)}$, CO evolves through path A (hydrogenation of $CO_2^{\bullet-}{}_{(ad)}$) or path B (reduction of $COOH_{(ad)}$). Water is photooxidized to form O_2 on the photocatalyst surface. Thus, adding a basic salt is key for efficient photocatalytic CO_2 reduction with smooth supply of hydrated CO_2 molecules.

3.3. Ag Cocatalyst-Loaded Photocatalysts for Single Particulate Photocatalytic CO_2 Reduction to Form CO

Various metal oxide photocatalysts with different components and crystal structure have been developed for CO_2 reduction based on loading Ag cocatalyst and adding $NaHCO_3$ strategies from our group as shown in Table 2, for example, $CaTa_4O_{11}$,[22] $LaTa_7O_{19}$,[22] and $KCaSrTa_5O_{15}$[23,24] photocatalysts. In addition, many metal oxide photocatalysts with wide band gaps have been reported for CO_2 reduction such as $La_2Ti_2O_7$,[25] $CaTiO_3$,[26] $SrTiO_3$:Al,[27] Ga_2O_3:Zn,[28] and $ZnGa_2O_4/Ga_2O_3$[29] with the Ag cocatalyst from other groups. Substitution of elements is also a beneficial approach to develop new photocatalysts for CO_2 reduction as well as for water splitting. For example, $KCaSrTa_5O_{15}$ (BG = 4.1 eV) has a tungsten bronze structure, which is similar to a defect type of perovskite structure ($A_{1-x}BO_3$). K, Ca, and Sr at an A site in $KCaSrTa_5O_{15}$ can be replaced with various other cations. $Sr_xK_yNa_zTa_5O_{15}$ and $K_2RETa_5O_{15}$ (RE = rear earth metal) obtained by the substitution are also active for photocatalytic CO_2 reduction.[30−32]

3.4. Rh−Ru Cocatalyst for CH_4 Formation by Photocatalytic CO_2 Reduction

Although many photocatalysts have been developed for CO_2 reduction as mentioned above, obtained products are limited to two-electron reduction products such as CO and HCOOH.

Table 3. Sacrificial CO_2 Reduction Using Metal Sulfide Photocatalysts under Visible Light Irradiation[19a]

metal sulfide	crystal structure	BG, EG [eV]	electron donor	activity [μmol h^{-1}]		
				H$_2$	CO	HCOOH
CuGaS$_2$	chalcopyrite	2.3	K$_2$SO$_3$	11	0.25	trace
(AgInS$_2$)$_{0.22}$–(ZnS)$_{1.56}$	wurtzite	2.3	Na$_2$S + K$_2$SO$_3$	16	0.01	0
(AgInS$_2$)$_{0.1}$–(ZnS)$_{1.8}$	wurtzite	2.6	Na$_2$S	23	0.06	0.10
Ag$_2$ZnGeS$_4$	stannite	2.5	Na$_2$S	38	0	0.14
ZnS:Ni(0.1%)	wurtzite + zinc blend	2.3	Na$_2$S	22	trace	4.0
ZnS:Pb(1.0%)	wurtzite + zinc blend	2.4	Na$_2$S	47	0.02	0.96
(ZnS)$_{0.9}$–(CuCl)$_{0.1}$	zinc blende	2.9	Na$_2$S	140	0.01	0
ZnGa$_{0.5}$In$_{1.5}$S$_4$	layered	2.7	Na$_2$S	14	0.01	0

[a]Photocatalyst, 0.2–0.3 g; reactant solution, 0.05–0.1 mol L^{-1} Na$_2$S or 0.1 mol L^{-1} K$_2$SO$_{3(aq)}$ (120–150 mL) or both; gas, CO_2 (1 atm); light source, 300 W Xe lamp (λ > 420 nm); irradiation area, 33 cm^2. BG = band gap, EG = energy gap.

Table 4. Z-Scheme Photocatalyst Systems for CO_2 Reduction Using Water as an Electron Donor under UV or Visible Light Irradiation[3,4,19,43,46a]

entry	reducing photocatalyst	O$_2$-evolving photocatalyst	mediator	additive (mmol L^{-1})	activity [μmol h^{-1}]			CO selectivity (%)	e$^-$/h$^+$
					H$_2$	O$_2$	CO		
1	CuGaS$_2$	RGO–TiO$_2$	RGO	none	28.8	11.2	0.15	0.5	1.29
2	CuGaS$_2$	RGO–(CoO$_x$/BiVO$_4$)	RGO	none	3.1	1.3	0.04	1.3	1.21
3	Cu$_{0.8}$Ag$_{0.2}$GaS$_2$	RGO–(CoO$_x$/BiVO$_4$)	RGO	NaHCO$_3$ (1)	4.0	1.6	0.03	0.7	1.26
4	CuGa$_{0.8}$In$_{0.2}$S$_2$	RGO–(CoO$_x$/BiVO$_4$)	RGO	NaHCO$_3$ (1)	3.5	1.6	0.04	1.1	1.11
5	(CuGa)$_{0.5}$ZnS$_2$	RGO–(CoO$_x$/BiVO$_4$)	RGO	NaHCO$_3$ (1)	3.5	1.9	0.4	11	1.04
6	(CuGa)$_{0.5}$ZnS$_2$	RGO–(CoO$_x$/BiVO$_4$)	RGO	NaHCO$_3$ (10)	12.0	6.4	1.8	13	1.08
7	(CuGa)$_{0.5}$ZnS$_2$	RGO–(CoO$_x$/BiVO$_4$)	RGO	KHCO$_3$ (10)	8.1	4.6	2.1	20	1.11
8	(CuGa)$_{0.5}$ZnS$_2$	RGO–(CoO$_x$/BiVO$_4$)	RGO	NaHCO$_3$ (100)	8.9	3.5	3.2	26	1.73
9	[Ru(dpbpy)]/(CuGa)$_{0.3}$Zn$_{1.4}$S$_2$	BiVO$_4$	Co[(tpy)$_2$]$^{3+/2+}$	NaHCO$_3$ (250)	1.7	0.8	2.7	56	3.00
10	SrTiO$_3$:Rh	BiVO$_4$	none	none	8.7	4.0	0.018	0.2	1.09
11	Au/SrTiO$_3$:Rh	BiVO$_4$	none	none	3.5	1.9	0.031	0.9	0.93

[a]Photocatalyst, 0.1–0.4 g; reactant solution, water (120–150 mL); flow gas, CO_2 (1 atm); light source, 300 W Xe lamp (λ > 300 nm for TiO$_2$ and λ > 420 nm for BiVO$_4$ systems); irradiation area, 33 cm^2.

Therefore, it is challenging to demonstrate CO_2 reduction to form CH$_4$, an eight-electron reduction product, using water as an electron donor. Rh–Ru/NaTaO$_3$:Sr(1%) continuously produces CH$_4$, H$_2$, and O$_2$ under UV irradiation.[33] The selectivity for CH$_4$ formation based on the number of reacted electrons is about 10%. The e$^-$/h$^+$ ratio estimated from obtained products is 1.1, and TON based on CH$_4$ formation with Rh and Ru cocatalysts is 2.0. No CH$_4$ is obtained under Ar rather than CO_2 flow. These results prove that CH$_4$ is obtained by photocatalytic CO_2 reduction using water as an electron donor over the Rh–Ru/NaTaO$_3$:Sr(1%).

4. Z-SCHEME CO_2 REDUCTION USING WATER AS AN ELECTRON DONOR UNDER VISIBLE LIGHT IRRADIATION (FIGURE 1b)

It is a key issue to construct visible light responsive CO_2 reduction system using water as an electron donor for efficient sunlight utilization beyond the wide band gap photocatalysts. In this section, visible light responsive photocatalysts for CO_2 reduction in the presence of a sacrificial electron donor (Table 3) and application of those photocatalysts to Z-scheme systems for CO_2 reduction using water as an electron donor under visible light (Table 4) are introduced.

4.1. Visible-Light Responsive Metal Sulfide Photocatalysts for CO_2 Reduction Using Sacrificial Electron Donor

Metal sulfide photocatalysts are active for not only water reduction but also CO_2 reduction under visible light using a sacrificial electron donor. For example, CdS is active for sacrificial CO_2 reduction to form CO in an aqueous solution containing a sacrificial reagent.[34,35] Metal sulfides with various crystal structures have also been developed for sacrificial CO_2 reduction under visible light irradiation as shown in Table 3.[19] CuGaS$_2$ and ZnS:Ni photocatalysts are highly active for CO and HCOOH formation, respectively. However, these CO_2 reductions are not artificial photosynthesis because strong sacrificial electron donors are used. Since they cannot oxidize water into O$_2$ because of self-photooxidation (photocorrosion), single particulate overall water splitting and CO_2 reduction accompanied by O$_2$ evolution by water oxidation as shown in Figure 1a is difficult. Construction of Z-scheme systems is a beneficial approach to employ metal sulfide photocatalysts showing CO_2 reduction activity combined with an O$_2$-evolving photocatalyst as shown in Figure 1b.

4.2. Z-Scheme System Employing RGO as a Solid-State Electron Mediator (Figure 4A(a))

A Z-scheme system consisting of CuGaS$_2$ as a reducing photocatalyst, TiO$_2$ as an O$_2$-evolving photocatalyst, and reduced graphene oxide (RGO) as a solid-state electron mediator is active for not only water splitting[36] but also CO_2 reduction to form CO (Table 4, entry 1).[19] The carbon source for the CO_2 reduction product should carefully be checked, because RGO is a carbon material. ^{13}CO formed under ^{13}CO$_2$ flow, indicating that flowed CO_2 was the carbon source. However, ^{12}CO was obtained in addition to the ^{13}CO.
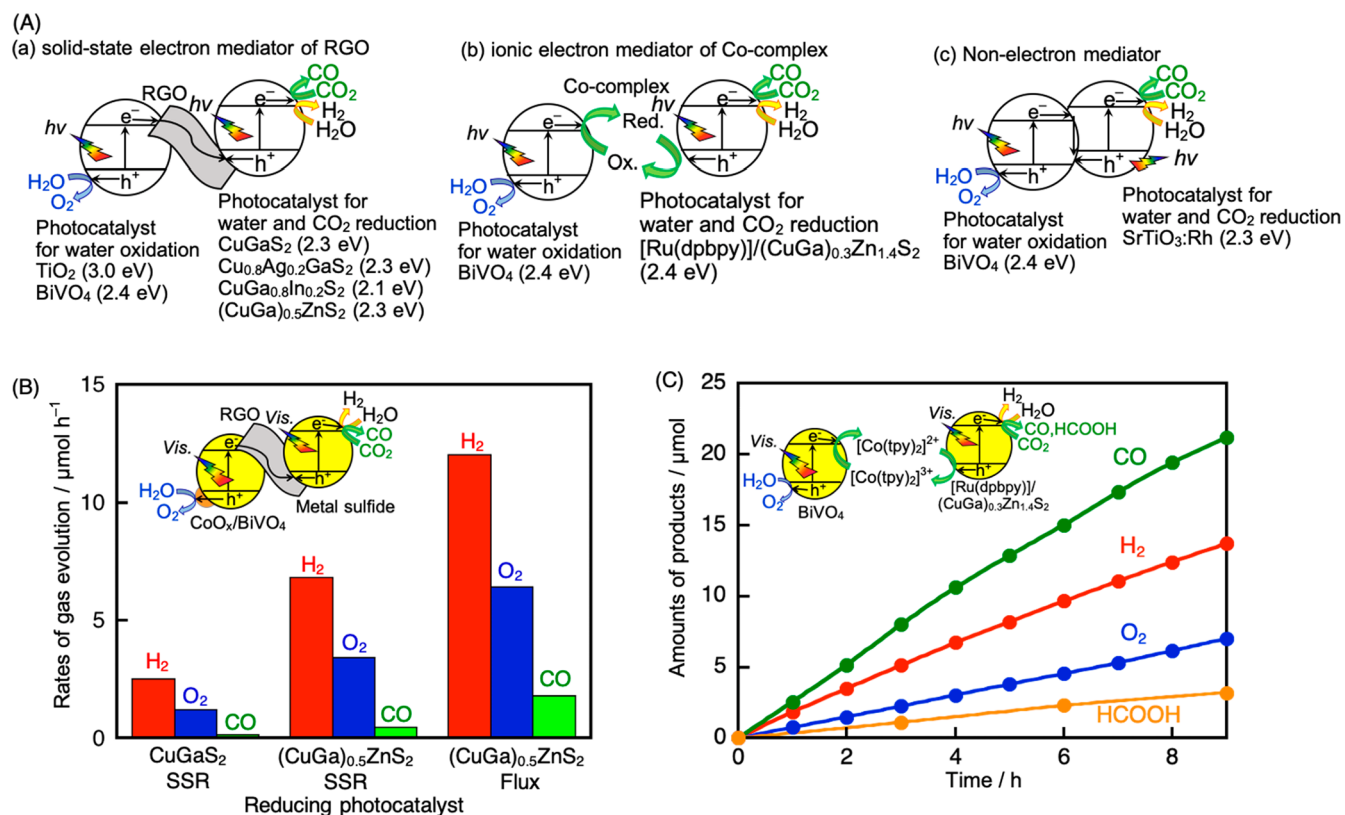
Figure 4. (A) Various types of Z-scheme photocatalysts for CO_2 reduction using water as an electron donor. (B) Z-scheme CO_2 reduction under visible light irradiation using $CuGaS_2$ or $(CuGa)_{0.5}ZnS_2$ prepared by a SSR or a flux method combined with $RGO-(CoO_x/BiVO_4)$. Reproduced with permission from ref 4. Copyright 2022 American Chemical Society. (C) Z-scheme CO_2 reduction under visible light irradiation using $[Ru(dpbby)]/(CuGa)_{0.3}Zn_{1.4}S_2$, $BiVO_4$, and $[Co(tpy)_2]^{3+/2+}$. Reproduced with permission from ref 43. Copyright 2018 The Royal Society of Chemistry. Photocatalyst, 0.1–0.4 g; reactant solution, $NaHCO_{3(aq)}$ (120–150 mL); flow gas, CO_2 (1 atm); light source, 300 W Xe lamp ($\lambda > 420$ nm); irradiation area, 33 cm^2.

Moreover, a small amount of CO formed even under Ar gas instead of CO_2. So, a part of CO formed by Z-scheme CO_2 reduction, whereas other CO formed by photooxidation of RGO on TiO_2. The Z-scheme system works only under UV light because of limitations of TiO_2. When visible light responsive $RGO-(CoO_x/BiVO_4)$ is employed instead of $RGO-TiO_2$, Z-scheme CO_2 reduction to form CO proceeds using water as an electron donor under visible light in an aqueous suspension (Table 4 entry 2).[3] CO is not obtained under Ar flow in the Z-scheme system composed of $RGO-(CoO_x/BiVO_4)$ unlike that using $RGO-TiO_2$. The inhibition of RGO oxidation is due to less oxidation power of holes photogenerated in the valence band of $BiVO_4$ than that of TiO_2.

Making a solid solution based on $CuGaS_2$ with p-type character is beneficial to developing a reducing photocatalyst, because the band structure is tunable by a change in the composition of the solid solution.[6,37] For example, solid solutions of $CuGaS_2$ with $CuInS_2$ can absorb longer wavelengths of visible light than $CuGaS_2$, because In 5s5p orbitals of $CuInS_2$ lower the conduction band consisting of Ga 4s4p orbitals of $CuGaS_2$ resulting in band gap narrowing. Red-powdered $CuGa_{0.8}In_{0.2}S_2$, which absorbs visible light up to 600 nm functions as a CO_2-reducing photocatalyst in the Z-scheme system (Table 4, entry 4). Making a $(CuGa)_{1-x}Zn_{2x}S_2$ solid solution between $CuGaS_2$ and ZnS improves $CuGaS_2$ performance, though the band gap does not become narrower than that of $CuGaS_2$.[38] The Z-scheme system using $(GuGa)_{0.5}ZnS_2$

prepared by a solid-state reaction (SSR) combined with $RGO-(CoO_x/BiVO_4)$ shows higher water splitting and CO_2 reduction activities than that using $CuGaS_2$ prepared by SSR (Figure 4B). When the $(CuGa)_{0.5}ZnS_2$ particle is prepared by a flux method, fine particles of $(CuGa)_{0.5}ZnS_2$ with a few hundreds of nanometers in size are obtained, while the particle size when prepared by conventional SSR is about 1 μm.[39] When the fine particulate $(CuGa)_{0.5}ZnS_2$ is applied to a Z-scheme system, photocatalytic water splitting and CO_2 reduction are much enhanced (Figure 4B).[4] The Z-scheme CO_2 reduction activity strongly depends on the reactant solution conditions (Table 4, entries 5−8). Addition of a basic salt not only stabilizes but also enhances Z-scheme CO_2 reduction because of efficient supply of hydrated CO_2 to the photocatalyst surface. We stress that the selectivity for CO formation in the Z-scheme CO_2 reduction reaches 10−20% even using bare metal sulfide without surface modification. Although a Ag cocatalyst is effective for CO_2 reduction to form CO over wide band gap metal oxides as mentioned in section 3, Ag on a metal sulfide does not enhance CO formation in the Z-scheme CO_2 reduction at the present stage, probably due to poisoning of the Ag surface by sulfurization. Therefore, further highly selective CO_2 reduction is expected by introducing a suitable active site and surface modification of the metal sulfide photocatalyst for Z-scheme CO_2 reduction.

4.3. Z-Scheme System Employing a Co-Complex as an Electron Mediator (Figure 4A(b))

Metal complexes have been widely examined as selective CO_2-reducing catalysts in electrochemistry, coordination chemistry, and photochemistry.[40,41] Recently, hybrid systems combining a metal complex catalyst with semiconductor photocatalyst materials have been studied for highly selective CO_2 reduction in photoelectrochemical and photocatalytic systems.[42] For example, Z-scheme CO_2 reduction under visible light has been demonstrated using [Ru(dpbpy)]-loaded $(CuGa)_{0.3}Zn_{1.4}S_2$, $BiVO_4$, and a Co-complex as an electron mediator (Figure 4C).[43] CO evolves as a main reduction product with introduction of the highly active Ru-complex catalyst for CO_2 reduction on $(CuGa)_{0.3}Zn_{1.4}S_2$. HCOOH is also produced in the reaction. The catalytic activity of a metal complex is usually inhibited in the presence of O_2. Therefore, it is notable that CO_2 reduction and simultaneous O_2 evolution proceed even using a metal complex catalyst with a semiconductor photocatalyst in an aqueous solution, though the amount of O_2 is small compared with a stoichiometric amount.

4.4. Z-Scheme System Driven by Interparticle Electron Transfer without an Electron Mediator (Figure 4A(c))

$SrTiO_3$:Rh shows high sacrificial H_2 evolution activity, though it does not oxidize water into O_2.[44] However, $SrTiO_3$:Rh can be employed to construct a Z-scheme system working via interparticle electron transfer with $BiVO_4$ without an electron mediator (Figure 4A(c)).[45,46] The Z-scheme system reduces CO_2 to CO accompanied by H_2 and O_2 under visible light. Loading Ag or Au cocatalyst on $SrTiO_3$:Rh improves the CO evolution activity (Table 4, entries 10, 11). The suitable pH is around 4, because $SrTiO_3$:Rh and $BiVO_4$ particles aggregate well with each other to get good contact between the particles, resulting in smooth electron transfer from $BiVO_4$ to $SrTiO_3$:Rh via interparticle electron transfer. It is notable that the Z-scheme CO_2 reduction proceeds using just photocatalyst powders, water, and CO_2 because of self-pH-adjustment by dissolved CO_2.

5. CO$_2$ REDUCTION ON p-TYPE Cu(I)-CONTAINING METAL SULFIDE PHOTOCATHODES UNDER VISIBLE LIGHT IRRADIATION (FIGURE 1c,d)

A photoelectrochemical CO_2 reduction system is also interesting to construct an artificial photosynthesis system. Photoelectrochemical measurement is generally conducted in a 3-electrode system or a 2-electrode system connected to a potentiostat and a power supply (Figure 5A). Scientifically intrinsic information on the working electrode, for example, an absolute electrode potential, is obtained with the 3-electrode system using a reference electrode. The 2-electrode system is useful for evaluation of cell performance such as open circuit voltage, short circuit current, and energy conversion efficiency. It is meaningless in a photoelectrochemical cell if an externally applied voltage is larger than the theoretical voltage of electrolysis, for example, 1.23 V for water splitting. Applying no external bias is ideal. To compare the performance of a photoelectrode, a current–potential curve is usually measured using the 3-electrode system. In addition, analysis of products by bulk electrolysis is also indispensable, as well as measurement of photocurrent to examine the Faradaic efficiency, that is, electrochemical selectivity. The Faradaic efficiency reveals if the photocurrent is due to desired redox reactions. Moreover,
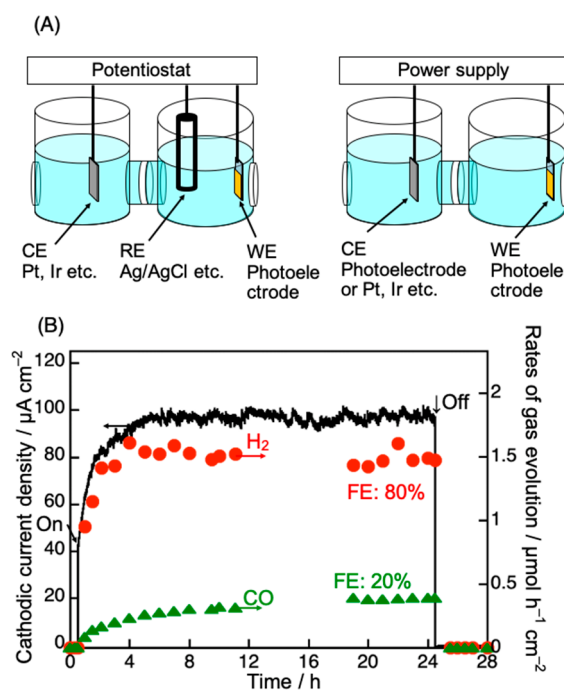

Figure 5. (A) Two-electrode and three-electrode systems for photoelectrochemical CO_2 reduction. (B) Photoelectrochemical CO_2 reduction under visible light irradiation over a $(CuGa)_{0.5}ZnS_2$ powder-based photocathode. Electrolyte, 0.1 mol L^{-1} $KHCO_{3(aq)}$; flow gas, CO_2 (1 atm); light source, 300 W Xe lamp ($\lambda > 420$ nm); applied bias, 0.1 V vs RHE (−0.5 V vs Ag/AgCl (pH 6.9)). Reproduced with permission from ref 4. Copyright 2022 American Chemical Society.

not only the Faradaic efficiency but also a partial photocurrent density (i.e., rate of production) are important to see how fast a certain product is formed. Incident photon to current conversion efficiency (IPCE) and solar energy conversion efficiency are also important.

The photoelectrochemical cell can employ p-type semiconductors as a photocathode even photocorrosive materials. For example, visible light responsive $CuGaS_2$,[47] $(CuGa)_{0.5}ZnS_2$,[4,38] $Cu_{0.8}Ag_{0.2}GaS_2$,[48,49] and Cu_2ZnGeS_4[50] function as a CO_2-reducing photocathodes. The bare $(CuGa)_{0.5}ZnS_2$ photocathode reduces CO_2 to CO with high stability under visible light with application of an external bias (Figure 5B).[4] Faradaic efficiencies for CO and H_2 formation are 20% and 80%, respectively, being almost 100% of total Faradaic efficiency. It is stressed that high CO formation is observed even without cocatalyst and surface modification on the photocathode.

Surface modification with CdS and ZnS of an n-type semiconductor and loading of a cocatalyst improve the performance of p-type $Cu_{0.8}Ag_{0.2}GaS_2$,[49] Cu_2ZnGeS_4,[51] and $(CuGa_{1-y}In_y)_{1-x}Zn_{2x}S_2$ solid solution[52] photocathodes. Introduction of an electrically conducting polymer such as polypyrrole (PPy) or poly(3,4-ethylenedioxythiophene) (PEDOT) as hole transporter also improves a photocathode composed of a powdered material, because electric contact between the powders and the substrate electrode such as FTO is usually poor.[53,54] PPy-modified $CuGaS_2$ gives higher cathodic photocurrent for water and CO_2 reduction than a bare $CuGaS_2$ photocathode. Moreover, the 2-electrode system combining a PEDOT−$CuGaS_2$ photocathode and a CoO_x/$BiVO_4$ photoanode with visible light response also reduces

CO_2 to CO using water as an electron donor under application of a small bias and simulated sunlight irradiation.

6. CONCLUSIONS AND PERSPECTIVES

Artificial photosynthesis is ideal green chemistry and technology to convert and store solar energy to chemical products as an uphill reaction. Solar water splitting to produce H_2 is representative of artificial photosynthesis. Solar water splitting using a powder-based photocatalyst on a large scale (100 m^2) has been demonstrated.[5] It will accelerate the industrial application of solar hydrogen production in the near future. In contrast to solar water splitting, artificial photosynthetic CO_2 utilization using photocatalysts is still at the stage of basic research. However, recent and rapid progress of this research area is hopeful. A variety of photocatalyst and photoelectrode systems for CO_2 utilization has been extensively developed using homogeneous and heterogeneous photocatalyst materials. This Account focused on photocatalytic and photoelectrochemical systems based on particulate photocatalysts for CO_2 reduction as an artificial photosynthesis system working under UV and visible light.

Highly active photocatalysts for water splitting such as $BaLa_4Ti_4O_{15}$ (BG = 3.9 eV) and doped $NaTaO_3$ (BG = 4.1 eV) were able to be applied to CO_2 reduction, because they have sufficiently high conduction bands and enough potential for water oxidation to form O_2. The O_2 evolution ability and a suitable cocatalyst working as a reaction center for CO_2 reduction are indispensable for photocatalytic CO_2 reduction using water as an electron donor. Ag and Rh–Ru cocatalysts were developed for CO and CH_4 formation, respectively. Moreover, the photocatalytic activity was increased with optimization of reaction conditions such as tuning of the reactant solution. Metal sulfide photocatalysts with a high conduction band and visible light response are attractive for CO_2 reduction, though they cannot oxidize water. This means that the metal sulfide photocatalyst itself cannot use water as an electron donor to achieve an uphill reaction. However, $CuGaS_2$, $(CuGa)_{1-x}Zn_{2x}S_2$, and $CuGa_{1-x}In_xS_2$ metal sulfide materials were able to be employed as a CO_2-reducing photocatalysts to make a Z-scheme photocatalyst system to achieve photocatalytic CO_2 reduction using water as an electron donor under visible light irradiation. p-Type metal sulfides $CuGaS_2$, $(CuGa)_{1-x}Zn_{2x}S_2$, and $Cu_{1-x}Ag_xGaS_2$ were able to be applied to a photocathode for photoelectrochemical CO_2 reduction, even if their powdered materials were employed.

Strategies to design photocatalytic and photoelectrochemical systems for CO_2 reduction using water as an electron donor under visible light irradiation become clearer as mentioned above. Therefore, it is expected that more efficient photocatalyst and photoelectrode systems can be developed with further extensive study. We believe that photocatalyst and photoelectrode systems for solar CO_2 utilization can be a practical use in the future as well as solar hydrogen production by water splitting.

■ AUTHOR INFORMATION

Corresponding Author

Akihiko Kudo − *Department of Applied Chemistry, Faculty of Science, Tokyo University of Science, Tokyo 162-8601, Japan;* ● orcid.org/0000-0002-5665-5482; Email: a-kudo@rs.tus.ac.jp

Authors

Shunya Yoshino − *Department of Applied Chemistry, Faculty of Science, Tokyo University of Science, Tokyo 162-8601, Japan;* ● orcid.org/0000-0002-5449-3379

Tomoaki Takayama − *Department of Applied Chemistry, Faculty of Science, Tokyo University of Science, Tokyo 162-8601, Japan;* Present Address: Department of Chemistry, School of Science, Tokyo Institute of Technology, Tokyo 152-8551, Japan

Yuichi Yamaguchi − *Department of Applied Chemistry, Faculty of Science, Tokyo University of Science, Tokyo 162-8601, Japan*

Akihide Iwase − *Department of Applied Chemistry, Faculty of Science, Tokyo University of Science, Tokyo 162-8601, Japan;* Present Address: Department of Applied Chemistry, School of Science and Technology, Meiji University, Kanagawa 214-8571, Japan; ● orcid.org/0000-0002-6395-9556

Complete contact information is available at:
https://pubs.acs.org/10.1021/acs.accounts.1c00676

Notes

The authors declare no competing financial interest.

Biographies

Shunya Yoshino is a postdoctoral researcher at Tokyo University of Science. He received his Ph.D. from Tokyo University of Science in 2021. His research focuses on Z-scheme and photoelectrochemical CO_2 reduction of artificial photosynthesis using metal sulfide photocatalysts.

Tomoaki Takayama is an assistant professor at Tokyo Institute of Technology. He received his Ph.D. from Tokyo University of Science in 2015 and worked as a postdoctoral researcher at Tokyo University of Science until 2017. Then, he joined Tokyo Institute of Technology as an assistant professor. His research interests include photocatalytic and photoelectrochemical CO_2 reduction over metal oxides and metal sulfides and intermetallic compound catalysis.

Yuichi Yamaguchi is an assistant professor at Tokyo University of Science. He received his Ph.D. from Tokyo University of Science in 2017 and worked as a postdoctoral researcher at Tokyo University of Science until 2018 and University of Liverpool from 2018 to 2019. He moved to Tokyo University of Science as an assistant professor. His current research interests include high frequency induction heating treatment of photocatalyst materials.

Akihide Iwase is an associate professor at Meiji University. He received his Ph.D. from Tokyo University of Science in 2009. He was a postdoctoral research associate at University of New South Wales in Australia from 2009 to 2012. Then, he joined Tokyo University of Science as an assistant professor from 2012 to 2019. He moved Meiji University in 2019 as an associate professor. His research interests involve Z-scheme systems using reduce graphene oxide for water splitting and CO_2 reduction. He also focuses on developing a photocatalyst with dopant for efficient water splitting.

Akihiko Kudo is a professor at Tokyo University of Science. He received a bachelor's degree from Tokyo University of Science in 1983 and Ph.D. from Tokyo Institute of Technology in 1988. After he was a postdoctoral fellow at University of Texas in Austin from 1988 to 1989, he worked as a research associate at Tokyo Institute of Technology until 1995. Then, he joined Tokyo University of Science as a Lecturer, became an associate professor in 1998, and became a full professor in 2003. His main interest is artificial photosynthesis for

water splitting, CO_2 reduction, and NH_3 decomposition over powdered semiconductor photocatalyst materials.

■ ACKNOWLEDGMENTS

■ REFERENCES

(1) Iizuka, K.; Wato, T.; Miseki, Y.; Saito, K.; Kudo, A. Photocatalytic Reduction of Carbon Dioxide over Ag Cocatalyst-Loaded $ALa_4Ti_4O_{15}$ (A = Ca, Sr, and Ba) Using Water as a Reducing Reagent. *J. Am. Chem. Soc.* **2011**, *133*, 20863−20868.

(2) Nakanishi, H.; Iizuka, K.; Takayama, T.; Iwase, A.; Kudo, A. Highly Active $NaTaO_3$-Based Photocatalysts for CO_2 Reduction to Form CO Using Water as the Electron Donor. *ChemSusChem* **2017**, *10*, 112−118.

(3) Iwase, A.; Yoshino, S.; Takayama, T.; Ng, Y. H.; Amal, R.; Kudo, A. Water Splitting and CO_2 Reduction under Visible Light Irradiation Using Z-Scheme Systems Consisting of Metal Sulfides, CoOx-Loaded $BiVO_4$, and a Reduced Graphene Oxide Electron Mediator. *J. Am. Chem. Soc.* **2016**, *138*, 10260−10264.

(4) Yoshino, S.; Iwase, A.; Yamaguchi, Y.; Suzuki, T. M.; Morikawa, T.; Kudo, A. Photocatalytic CO_2 Reduction Using Water as an Electron Donor under Visible Light Irradiation by Z-Scheme and Photoelectrochemical Systems over $(CuGa)_{0.5}ZnS_2$ in the Presence of Basic Additives. *J. Am. Chem. Soc.* **2022**, *144*, 2323−2332.

(5) Nishiyama, H.; Yamada, T.; Nakabayashi, M.; Maehara, Y.; Yamaguchi, M.; Kuromiya, Y.; Nagatsuma, Y.; Tokudome, H.; Akiyama, S.; Watanabe, T.; Narushima, R.; Okunaka, S.; Shibata, N.; Takata, T.; Hisatomi, T.; Domen, K. Photocatalytic Solar Hydrogen Production from Water on a 100-m^2 Scale. *Nature* **2021**, *598*, 304−307.

(6) Kudo, A.; Miseki, Y. Heterogeneous Photocatalyst Materials for Water Splitting. *Chem. Soc. Rev.* **2009**, *38*, 253−278.

(7) Hisatomi, T.; Kubota, J.; Domen, K. Recent Advances in Semiconductors for Photocatalytic and Photoelectrochemical Water Splitting. *Chem. Soc. Rev.* **2014**, *43*, 7520−7535.

(8) Chen, S.; Takata, T.; Domen, K. Particulate Photocatalysts for Overall Water Splitting. *Nat. Rev. Mater.* **2017**, *2*, 17050.

(9) Wang, Q.; Domen, K. Particulate Photocatalysts for Light-Driven Water Splitting: Mechanisms, Challenges, and Design Strategies. *Chem. Rev.* **2020**, *120*, 919−985.

(10) Bard, A. J. Photoelectrochemistry and Heterogeneous Photo-Catalysis at Semiconductors. *J. Photochem.* **1979**, *10*, 59−75.

(11) Kudo, A. Z-Scheme Photocatalyst Systems for Water Splitting under Visible Light Irradiation. *MRS Bull.* **2011**, *36*, 32−38.

(12) Maeda, K. Z-Scheme Water Splitting Using Two Different Semiconductor Photocatalysts. *ACS Catal.* **2013**, *3*, 1486−1503.

(13) Wang, Y.; Suzuki, H.; Xie, J.; Tomita, O.; Martin, D. J.; Higashi, M.; Kong, D.; Abe, R.; Tang, J. Mimicking Natural Photosynthesis: Solar to Renewable H_2 Fuel Synthesis by Z-Scheme Water Splitting Systems. *Chem. Rev.* **2018**, *118*, 5201−5241.

(14) Yui, T.; Kan, A.; Saitoh, C.; Koike, K.; Ibusuki, T.; Ishitani, O. Photochemical Reduction of CO_2 Using TiO_2: Effects of Organic

(15) Sayama, K.; Arakawa, H. Photocatalytic Decomposition of Water and Photocatalytic Reduction of Carbon Dioxide over Zirconia Catalyst. *J. Phys. Chem.* **1993**, *97*, 531−533.

(16) Miseki, Y.; Kato, H.; Kudo, A. Water Splitting into H_2 and O_2 over Niobate and Titanate Photocatalysts with (111) Plane-Type Layered Perovskite Structure. *Energy Environ. Sci.* **2009**, *2*, 306−314.

(17) Hori, Y.; Wakebe, H.; Tsukamoto, T.; Koga, O. Electrocatalytic Process of CO Selectivity in Electrochemical Reduction of CO_2 at Metal Electrodes in Aqueous Media. *Electrochim. Acta* **1994**, *39*, 1833−1839.

(18) Hori, Y. Electrochemical CO_2 Reduction on Metal Electrodes. In *Modern Aspects of Electrochemistry*; Vayenas, C. G., White, R. E., Gamboa-Aldeco, M. E., Eds.; Springer: New York, 2008; pp 89−189.

(19) Takayama, T.; Sato, K.; Fujimura, T.; Kojima, Y.; Iwase, A.; Kudo, A. Photocatalytic CO_2 Reduction Using Water as an Electron Donor by a Powdered Z-Scheme System Consisting of Metal Sulfide and an RGO−TiO_2 Composite. *Faraday Discuss.* **2017**, *198*, 397−407.

(20) Kato, H.; Asakura, K.; Kudo, A. Highly Efficient Water Splitting into H_2 and O_2 over Lanthanum-Doped $NaTaO_3$ Photocatalysts with High Crystallinity and Surface Nanostructure. *J. Am. Chem. Soc.* **2003**, *125*, 3082−3089.

(21) Iwase, A.; Kato, H.; Kudo, A. The Effect of Alkaline Earth Metal Ion Dopants on Photocatalytic Water Splitting by $NaTaO_3$ Powder. *ChemSusChem* **2009**, *2*, 873−877.

(22) Takayama, T.; Nakanishi, H.; Matsui, M.; Iwase, A.; Kudo, A. Photocatalytic CO_2 Reduction Using Water as an Electron Donor over Ag-Loaded Metal Oxide Photocatalysts Consisting of Several Polyhedra of Ti^{4+}, Zr^{4+}, and Ta^{5+}. *J. Photochem. Photobiol. A Chem.* **2018**, *358*, 416−421.

(23) Takayama, T.; Tanabe, K.; Saito, K.; Iwase, A.; Kudo, A. The $KCaSrTa_5O_{15}$ Photocatalyst with Tungsten Bronze Structure for Water Splitting and CO_2 Reduction. *Phys. Chem. Chem. Phys.* **2014**, *16*, 24417−24422.

(24) Takayama, T.; Iwase, A.; Kudo, A. Photocatalytic Water Splitting and CO_2 Reduction over $KCaSrTa_5O_{15}$ Nanorod Prepared by a Polymerized Complex Method. *Bull. Chem. Soc. Jpn.* **2015**, *88*, 538−543.

(25) Wang, Z.; Teramura, K.; Hosokawa, S.; Tanaka, T. Photo-catalytic Conversion of CO_2 in Water over Ag-Modified $La_2Ti_2O_7$. *Appl. Catal. B Environ.* **2015**, *163*, 241−247.

(26) Yoshida, H.; Zhang, L.; Sato, M.; Morikawa, T.; Kajino, T.; Sekito, T.; Matsumoto, S.; Hirata, H. Calcium Titanate Photocatalyst Prepared by a Flux Method for Reduction of Carbon Dioxide with Water. *Catal. Today* **2015**, *251*, 132−139.

(27) Wang, S.; Teramura, K.; Hisatomi, T.; Domen, K.; Asakura, H.; Hosokawa, S.; Tanaka, T. Effective Driving of Ag-Loaded and Al-Doped $SrTiO_3$ under Irradiation at $\lambda > 300$nm for the Photocatalytic Conversion of CO2 by H2O. *ACS Appl. Energy Mater.* **2020**, *3*, 1468−1475.

(28) Teramura, K.; Wang, Z.; Hosokawa, S.; Sakata, Y.; Tanaka, T. A Doping Technique That Suppresses Undesirable H_2 Evolution Derived from Overall Water Splitting in the Highly Selective Photocatalytic Conversion of CO_2 in and by Water. *Chem. - A Eur. J.* **2014**, *20*, 9906−9909.

(29) Wang, Z.; Teramura, K.; Huang, Z.; Hosokawa, S.; Sakata, Y.; Tanaka, T. Tuning the Selectivity toward CO Evolution in the Photocatalytic Conversion of CO_2 with H_2O through the Modification of Ag-Loaded Ga_2O_3 with a $ZnGa_2O_4$ Layer. *Catal. Sci. Technol.* **2016**, *6*, 1025−1032.

(30) Huang, Z.; Teramura, K.; Hosokawa, S.; Tanaka, T. Fabrication of Well-Shaped $Sr_2KTa_5O_{15}$ Nanorods with a Tetragonal Tungsten Bronze Structure by a Flux Method for Artificial Photosynthesis. *Appl. Catal. B Environ.* **2016**, *199*, 272−281.

(31) Huang, Z.; Yoshizawa, S.; Teramura, K.; Asakura, H.; Hosokawa, S.; Tanaka, T. Sodium Cation Substitution in $Sr_2KTa_5O_{15}$

toward Enhancement of Photocatalytic Conversion of CO_2 Using H_2O as an Electron Donor. *ACS Omega* **2017**, 2, 8187−8197.

(32) Huang, Z.; Teramura, K.; Asakura, H.; Hosokawa, S.; Tanaka, T. Flux Method Fabrication of Potassium Rare-Earth Tantalates for CO_2 Photoreduction Using H_2O as an Electron Donor. *Catal. Today* **2018**, 300, 173−182.

(33) Soontornchaiyakul, W.; Yoshino, S.; Yamaguchi, Y.; Kudo, A. *Abstracts of Papers, 129th CATSJ Meeting, Kyoto, Japan* 2022, P122.

(34) Fujiwara, H.; Hosokawa, H.; Murakoshi, K.; Wada, Y.; Yanagida, S.; Okada, T.; Kobayashi, H. Effect of Surface Structures on Photocatalytic CO_2 Reduction Using Quantized CdS Nanocrystallites. *J. Phys. Chem. B* **1997**, 101, 8270−8278.

(35) Kanemoto, M.; Ankyu, H.; Wada, Y.; Yanagida, S. Visible-Light Induced Photofixation of CO_2 into Benzophenone Catalyzed by Colloidal CdS Microcrystallites. *Chem. Lett.* **1992**, 21, 2113−2114.

(36) Iwashina, K.; Iwase, A.; Ng, Y. H.; Amal, R.; Kudo, A. Z-Schematic Water Splitting into H_2 and O_2 Using Metal Sulfide as a Hydrogen-Evolving Photocatalyst and Reduced Graphene Oxide as a Solid-State Electron Mediator. *J. Am. Chem. Soc.* **2015**, 137, 604−607.

(37) Kudo, A.; Kato, H.; Tsuji, I. Strategies for the Development of Visible-Light-Driven Photocatalysts for Water Splitting. *Chem. Lett.* **2004**, 33, 1534−1539.

(38) Kato, T.; Hakari, Y.; Ikeda, S.; Jia, Q.; Iwase, A.; Kudo, A. Utilization of Metal Sulfide Material of $(CuGa)_{1-X}Zn_{2X}S_2$ Solid Solution with Visible Light Response in Photocatalytic and Photoelectrochemical Solar Water Splitting Systems. *J. Phys. Chem. Lett.* **2015**, 6, 1042−1047.

(39) Yoshino, S.; Iwase, A.; Ng, Y. H.; Amal, R.; Kudo, A. Z-Schematic Solar Water Splitting Using Fine Particles of H_2-Evolving $(CuGa)_{0.5}ZnS_2$ Photocatalyst Prepared by a Flux Method with Chloride Salts. *ACS Appl. Energy Mater.* **2020**, 3, 5684−5692.

(40) Yamazaki, Y.; Takeda, H.; Ishitani, O. Photocatalytic Reduction of CO_2 Using Metal Complexes. *J. Photochem. Photobiol. C Photochem. Rev.* **2015**, 25, 106−137.

(41) Wang, W.; Himeda, Y.; Muckerman, J. T.; Manbeck, G. F.; Fujita, E. CO_2 Hydrogenation to Formate and Methanol as an Alternative to Photo- and Electrochemical CO_2 Reduction. *Chem. Rev.* **2015**, 115, 12936−12973.

(42) Maeda, K. Metal-Complex/Semiconductor Hybrid Photocatalysts and Photoelectrodes for CO_2 Reduction Driven by Visible Light. *Adv. Mater.* **2019**, 31, 1808205.

(43) Suzuki, T. M.; Yoshino, S.; Takayama, T.; Iwase, A.; Kudo, A.; Morikawa, T. Z-Schematic and Visible-Light-Driven CO_2 Reduction Using H_2O as an Electron Donor by a Particulate Mixture of a Ru-Complex/$(CuGa)_{1-x}Zn_{2x}S_2$ Hybrid Catalyst, $BiVO_4$ and an Electron Mediator. *Chem. Commun.* **2018**, 54, 10199−10202.

(44) Konta, R.; Ishii, T.; Kato, H.; Kudo, A. Photocatalytic Activities of Noble Metal Ion Doped $SrTiO_3$ under Visible Light Irradiation. *J. Phys. Chem. B* **2004**, 108, 8992−8995.

(45) Sasaki, Y.; Nemoto, H.; Saito, K.; Kudo, A. Solar Water Splitting Using Powdered Photocatalysts Driven by Z-Schematic Interparticle Electron Transfer without an Electron Mediator. *J. Phys. Chem. C* **2009**, 113, 17536−17542.

(46) Yoshino, S.; Sato, K.; Yamaguchi, Y.; Iwase, A.; Kudo, A. Z-Schematic CO_2 Reduction to CO through Interparticle Electron Transfer between $SrTiO_3$:Rh of a Reducing Photocatalyst and $BiVO_4$ of a Water Oxidation Photocatalyst under Visible Light. *ACS Appl. Energy Mater.* **2020**, 3, 10001−10007.

(47) Ikeda, S.; Tanaka, Y.; Kawaguchi, T.; Fujikawa, S.; Harada, T.; Takayama, T.; Iwase, A.; Kudo, A. Photoelectrochemical Reduction of CO_2 to CO Using a $CuGaS_2$ Thin-Film Photocathode Prepared by a Spray Pyrolysis Method. *Chem. Lett.* **2018**, 47, 1424−1427.

(48) Kaga, H.; Tsutsui, Y.; Nagane, A.; Iwase, A.; Kudo, A. An Effect of Ag(I)-Substitution at Cu Sites in $CuGaS_2$ on Photocatalytic and Photoelectrochemical Properties for Solar Hydrogen Evolution. *J. Mater. Chem. A* **2015**, 3, 21815−21823.

(49) Takayama, T.; Iwase, A.; Kudo, A. *Abstracts of Papers, 114th CATSJ Meeting Hiroshima, Japan*; 2014, 1D05.

(50) Ikeda, S.; Fujikawa, S.; Harada, T.; Nguyen, T. H.; Nakanishi, S.; Takayama, T.; Iwase, A.; Kudo, A. Photocathode Characteristics of a Spray-Deposited Cu_2ZnGeS_4 Thin Film for CO_2 Reduction in a CO_2-Saturated Aqueous Solution. *ACS Appl. Energy Mater.* **2019**, 2, 6911−6918.

(51) Kamimura, S.; Sasaki, Y.; Kanaya, M.; Tsubota, T.; Ohno, T. Improvement of Selectivity for CO_2 Reduction by Using Cu_2ZnSnS_4 Electrodes Modified with Different Buffer Layers (CdS and In_2S_3) under Visible Light Irradiation. *RSC Adv.* **2016**, 6, 112594−112601.

(52) Hayashi, T.; Niishiro, R.; Ishihara, H.; Yamaguchi, M.; Jia, Q.; Kuang, Y.; Higashi, T.; Iwase, A.; Minegishi, T.; Yamada, T.; Domen, K.; Kudo, A. Powder-Based $(CuGa_{1-y}In_y)_{1-x}Zn_{2x}S_2$ Solid Solution Photocathodes with a Largely Positive Onset Potential for Solar Water Splitting. *Sustain. Energy Fuels* **2018**, 2, 2016−2024.

(53) Takayama, T.; Iwase, A.; Kudo, A. *Abstracts of Papers, 96th CSJ Annual Meeting, Kyoto, Japan*; 2016, 1B1-44.

(54) Takayama, T.; Iwase, A.; Kudo, A. *Abstracts of Papers, 118th CATSJ Meeting, Iwate, Japan*; 2016, 3I11.

■ NOTE ADDED AFTER ASAP PUBLICATION

This paper was published on March 1, 2022. Due to production error, a value in Table 4 was incorrect. The corrected version was reposted on March 2, 2022.